John Cranor
EP2/53

REPORT NO. GDSS-CRAD-87-00

DESIGN AND DEMONSTRATE THE PERFORMANCE OF CRYOGENIC COMPONENTS REPRESENTATIVE OF SPACE VEHICLES

START BASKET LIQUID ACQUISITION DEVICE PERFORMANCE ANALYSIS

February 1987

Prepared Under
Contract NAS8-31778

Prepared for
NATIONAL AERONAUTICS AND SPACE ADMINISTRATION
George C. Marshall Space Flight Center
Marshall Space Flight Center, Alabama 35812

Prepared by
GENERAL DYNAMICS SPACE SYSTEMS DIVISION
P. O. Box 85990
San Diego, California 92138

FOREWORD

This report was prepared by General Dynamics Space Systems Division (GDSS) under NASA Marshall Space Flight Center Contract NAS8-31778.

This report documents the results of the final phase of the technical effort to Design and Demonstrate the Performance of Cryogenic Components Representative of Space Vehicles. The NASA/MSFC Program Manager for this phase of the contract was Mr. John Cramer. The important contributions made to this effort by Mr. Cramer are gratefully acknowledged.

The GDSS Study Manager for this final phase of the program was Mr. Franklin O. Bennett, Jr. Significant contributions to the analysis of start basket performance were made by Dr. In-Kun Kim and Mr. Mark A. Wollen.

TABLE OF CONTENTS

LIST OF FIGURES

LIST OF TABLES

LIST OF SYMBOLS

Roman	Definition
D_{BP}	Screen bubble point diameter
g	Gap width, Acceleration
h,H	Height
P	Pressure
ΔP	Pressure difference
r	Radius

Greek	
Θ	Contact angle
ρ	Density
σ	Liquid surface tension
ϕ	Screen wicking constant

Subscript	
a	Ambient
l	Liquid
ret	Retention
s	Screen
u	Ullage

ACRONYMS AND ABBREVIATIONS

CBT	Cryogenic Breadboard Tank
CFMFE	Cryogenic Fluid Management Flight Experiment
GH_2	Gaseous Hydrogen
GHe	Gaseous Helium
GPM	Gallons per Minute
IRAD	Independent Research and Development
LAD	Liquid Acquisition Device
LH_2	Liquid Hydrogen
LTCSF	Long Term Cryogenic Storage Facility
MLI	Multilayer Insulation
NBP	Normal Boiling Point
OTV	Orbital Transfer Vehicle
PPO	Polyphenylene Oxide
R&D	Research and Development
SBOTV	Space-Based Orbital Transfer Vehicle
SSP	Space Station Program
TVS	Thermodynamic Vent System

SUMMARY

The objective of this program was to design, fabricate, and test an integrated cryogenic test article incorporating both fluid and thermal propellant management subsystems. A 2.2-m (87-in.) diameter aluminum test tank was outfitted with multilayer insulation, helium purge system, low-conductive tank supports, thermodynamic vent system, liquid acquisition device, and immersed outflow pump. This report documents tests and analyses performed on the start basket liquid acquisition device, and related studies of the liquid retention characteristics of fine mesh screens.

SECTION 1

INTRODUCTION

The evolution of reusable, cryogenic, space-based orbital transfer vehicles and propellant storage depots will require the development and integration of multiple technologies in the field of zero-gravity liquid propellant management. The purpose of this contract was to design, fabricate, and test an integrated, prototypical, flightweight, test article incorporating as many of these technologies as possible. The test article consisted of an aluminum tank with multilayer insulation (MLI), an insulation purge bag and helium purge system, low-conductive tank support struts, zero-g thermodynamic vent system (TVS) with fluid mixer, start basket liquid acquisition device (LAD), immersed cryogenic outflow pump, warm and cold gas (hydrogen or helium) tank pressurization system, and sufficient internal and external instrumentation to permit evaluation of system performance.

Phase I of the program involved the development of a low-cost, organically-coated aluminized Kapton MLI system as an alternative to the expensive goldized Kapton systems used previously. Details of this work are documented in the Phase I report (Ref. 1). The second phase included MLI and purge system design and fabrication, zero-g TVS integration, start basket LAD design and fabrication, pump/feed system design integration, instrumentation design, and system level thermal performance analyses. This work is described in Ref. 2, the Phase II report.

The completed test article was packaged and shipped to the Marshall Space Flight Center in December 1981. Unavailability of the large vacuum test facility postponed initiation of testing until March of 1984. A number of tanking and outflow tests were performed in 1984 and data were obtained on start basket performance. Repeated attempts to achieve a hard vacuum under cryogenic conditions were made in 1984 and 1985 with limited success. Small leaks in the aluminum tank and fluid connections when chilled to liquid hydrogen temperature were encountered, isolated, and repaired. These and other hardware problems extended the test program to the point that the vacuum facility was required for higher priority work. The test program was terminated and the test article was removed from the chamber in late 1985.

The final phase of the contract statement of work was modified to delete MSFC test support and substitute an analysis of the start basket test data. This report documents that work.

SECTION 2

TEST ARTICLE DESCRIPTION

2.1 INTRODUCTION

The hydrogen propellant management test article, called the "Cryogenic Breadboard Tank" (CBT) by MSFC, was designed to serve as a test bed for the evaluation of cryogenic propellant management system components representative of future orbital transfer vehicles and space-based propellant storage depots. An existing large scale, flightweight tank was selected to serve as the means of integrating various fluid and thermal management subsystems located both inside and outside the tank. The propellant management subsystems selected for incorporation into the test article included MLI, a purge bag and purge gas distribution system, support struts, start basket LAD, TVS with fluid mixer, and outflow pump. The system can be pressurized with either warm or cold hydrogen or helium gas. The completed test article is shown schematically in Figure 2-1. The components are described in detail in References 1 and 2, and are summarized in this section.

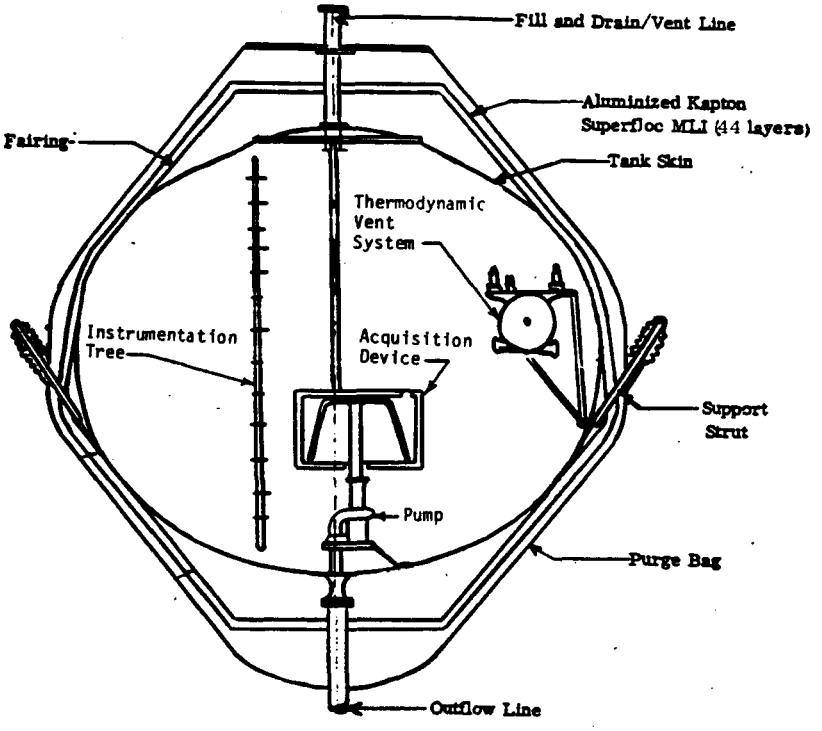

Figure 2-1. Cross-Sectional Schematic of the CBT

2.2 TANK

The tank is a 2.2 x 1.9-m (87 x 75-in.) diameter oblate spheroid fabricated from 2219-T62 aluminum. It has a surface area of 14.1 m^2 (152 ft^2), volume of 5 m^3 (175 ft^3), and chem milled wall thickness ranging from 1.95 to 3.94 mm (0.077 to 0.155 in.). The tank contains external bracketry for six pairs of support struts arranged in "V" patterns, a drain penetration at the bottom, and a 0.61-m (24-in.) access opening on the top (Figure 2-2). The access cover has provisions for nine electrical passthroughs and four fluid connections. The fill/drain/vent line consists of co-axial tubes to help reduce heat flow from the external environment. Draining can also be achieved by activating the outflow pump and flowing out the bottom penetration. The tank is installed in a black cylindrical enclosure which protects the fragile MLI from handling damage, provides a uniform radiation source temperature for high vacuum thermal performance testing, and which serves as a base for mounting heat lamps for elevated temperature testing. The aluminum tank was designed and built in the mid-1960's as a test bed for cryogenic propellant management system components. It has been insulated three times with three different Superfloc MLI system configurations, once on an internal R&D program and twice on contracted studies, and twice tested at vacuum levels approaching 133 μPa (1.0 x 10^{-6} torr).

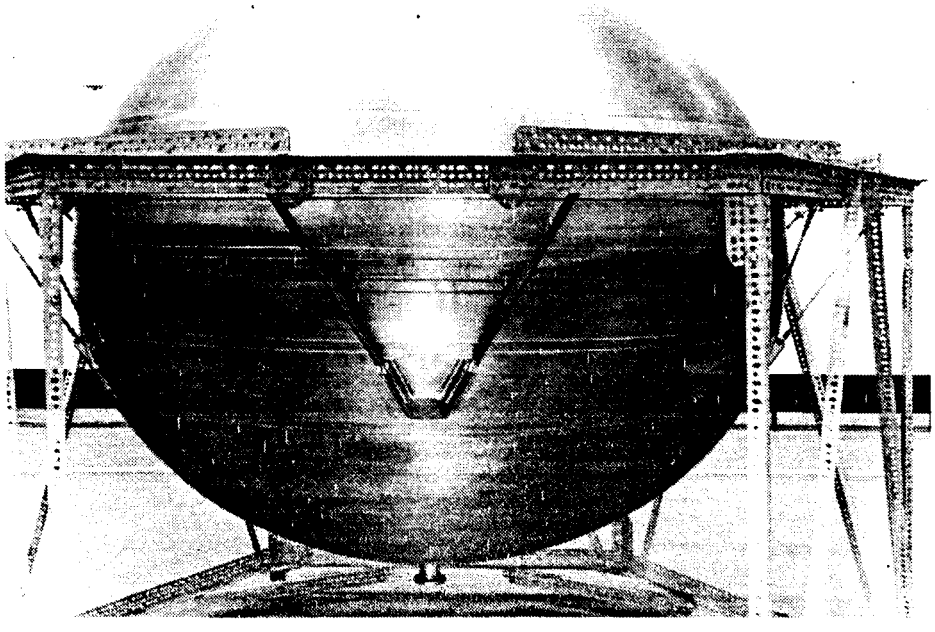

Figure 2-2. Aluminum Test Tank in Handling Fixture

2.3 EXTERNAL COMPONENTS

Due to the severity of the tank curvature, a fiberglass fairing system was designed to fit over the exterior of the tank and serve both as a mounting surface for the multilayer insulation system and as an internal plenum for the helium purge system. The outline of the fairing system is shown in Figure 2-1. The MLI system consists of 44 layers of organically coated, double aluminized Kapton Superfloc installed in two 1.9-cm (0.75-in.) thick blanket layers. Each blanket layer has twelve gore sections held together by polyphenylene oxide (PPO) grommets, and attached to each other by molded PPO twin pins. Slotted purge pins mounted on the fairing penetrate the MLI and distribute purge gas uniformly between the layers.

The tank/insulation system is enclosed in a two-piece, rigid purge bag constructed of glass cloth preimpregnated with epoxy resin and covered with layers of FEP teflon. A penetration panel located on top of the bag has provisions to handle the fluid and electrical lines from the tank cover. A 15.25-cm (6.0-in.) motorized butterfly valve mounted on top of the bag is used to vent the purge gases.

Three pairs of struts are used to support the tank from the enclosure. The struts are epoxy/fiberglass tubes with stainless steel spools and spherical ball fittings at each end. The hollow tubes are filled with Superfloc MLI disks to reduce radiation tunneling to the cold end of the strut. These highly-efficient tank supports are estimated to contribute only four percent of the total heat leak to the tank (Ref. 2). The contributions of all the heat leak components are summarized in Figure 2-3. An external view of the fully insulated tank is shown in Figure 2-4.

2.4 INTERNAL COMPONENTS

The principal internal fluid management components are the start basket liquid acquisition device, a thermodynamic vent system with fluid mixer, and a submersible liquid hydrogen outflow pump. The start basket will be described in Section 3 where the test data analysis is presented.

The TVS used in this system was that developed by General Dynamics under Contract NAS8-20146. It is designed to control tank pressure while preventing the expulsion of liquid propellant from the tank in a zero-gravity environment. The unit is sized for a vent flow rate of 0.95 gm/s (3.0 lbm/hr). For testing purposes, either liquid or vapor can be passed into the cold side of the device by altering the setting of the selection valve. The fluid is then passed through

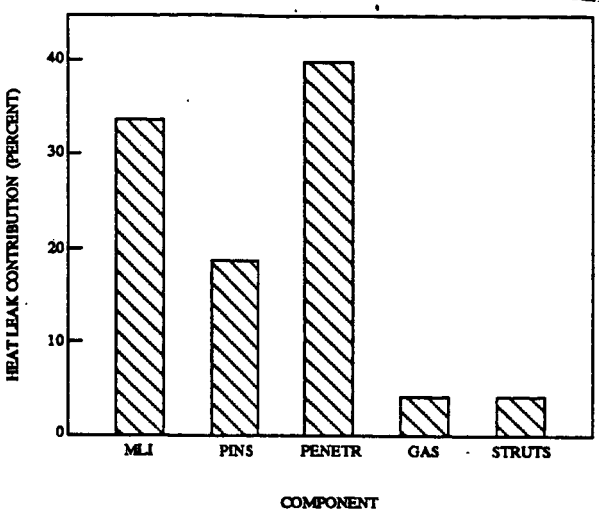

Figure 2-3. Estimated Component Heat Leak Contributions

Figure 2-4. Tank Insulated with Superfloc MLI Blankets

a filter and a regulating valve where it is throttled to near vacuum conditions. The thermodynamically cooled fluid then flows through the cold side of an internal tank heat exchanger. Relatively warm tank fluid is pumped through the hot side, and heat exchange vaporizes and warms the venting fluid while it cools the tank fluid. A similar TVS was developed for the liquid hydrogen tank of the Centaur G and G-Prime upper stage vehicles which were designed to be launched in the Shuttle cargo bay. A schematic of the TVS components is shown in Figure 2-5.

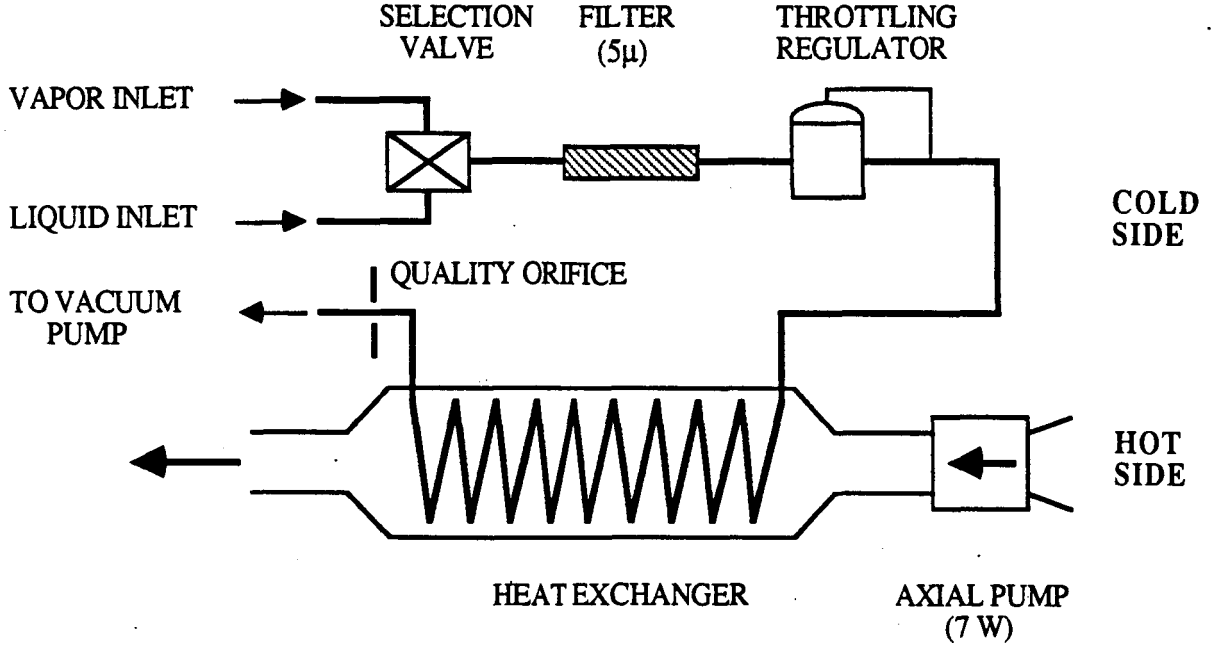

Figure 2-5. Thermodynamic Vent System Components

The outflow pump is a production recirculation unit developed for the Saturn program. It was supplied to this program as government furnished equipment. It draws 790 W of power and has a design flow rate of 8.5 $m(m^3)/s$ (135 GPM). It is mounted directly underneath, and draws liquid from, the start basket.

The tank contains an instrumentation tree with platinum resistance temperature devices and government-furnished capacitance-type liquid level sensors from the External Tank program. A continuous capacitance probe installed next to the basket measures tank fill level. The start basket also has two capacitance liquid level sensors, one each in the inner and outer volumes.

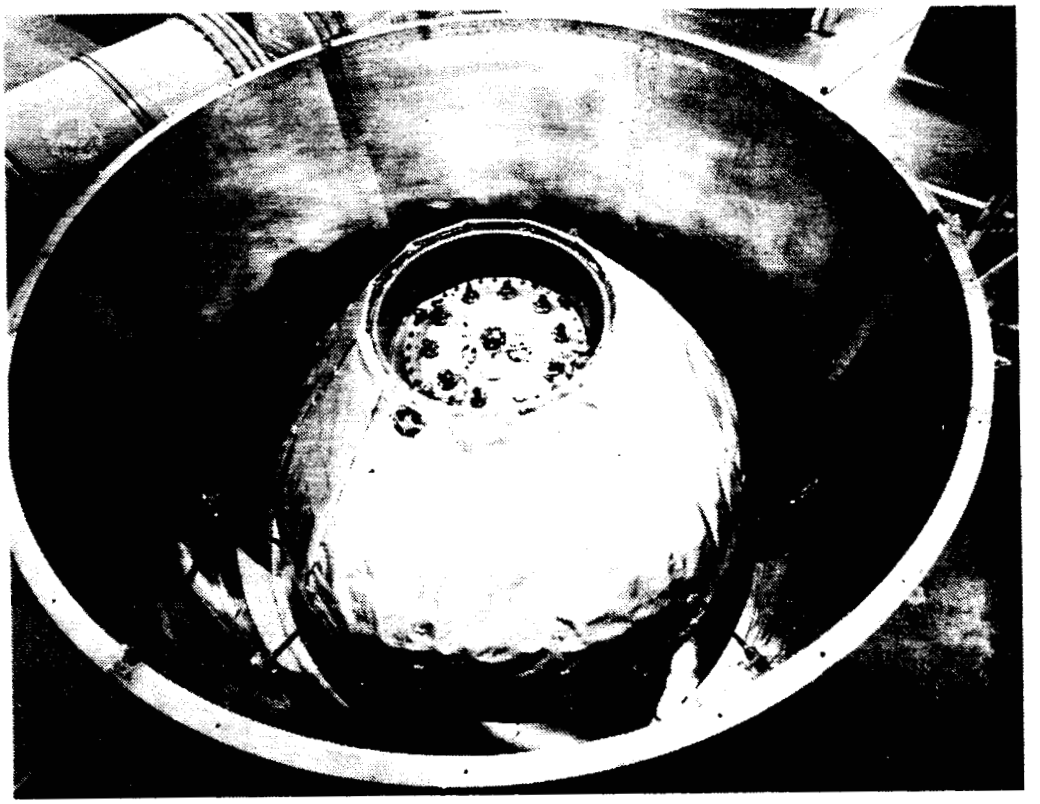

Figure 2-6. Insulated Tank Mounted in Enclosure

All instrumentation and electrical leads pass through the top access cover shown in Figure 2-6.

2.5 ASSEMBLY AND SHIPPING

Final assembly of the CBT system was performed at the General Dynamics Liquid Hydrogen Test Center in Sycamore Canyon. Figure 2-7 shows the final installation of the tankage system in the cylindrical enclosure. A special shipping crate was designed and fabricated to protect the system. Instrumentation was installed inside the crate to measure acceleration loading. The crated tank/enclosure was installed on a flat bed truck (Figure 2-8) and transported to MSFC in December 1981.

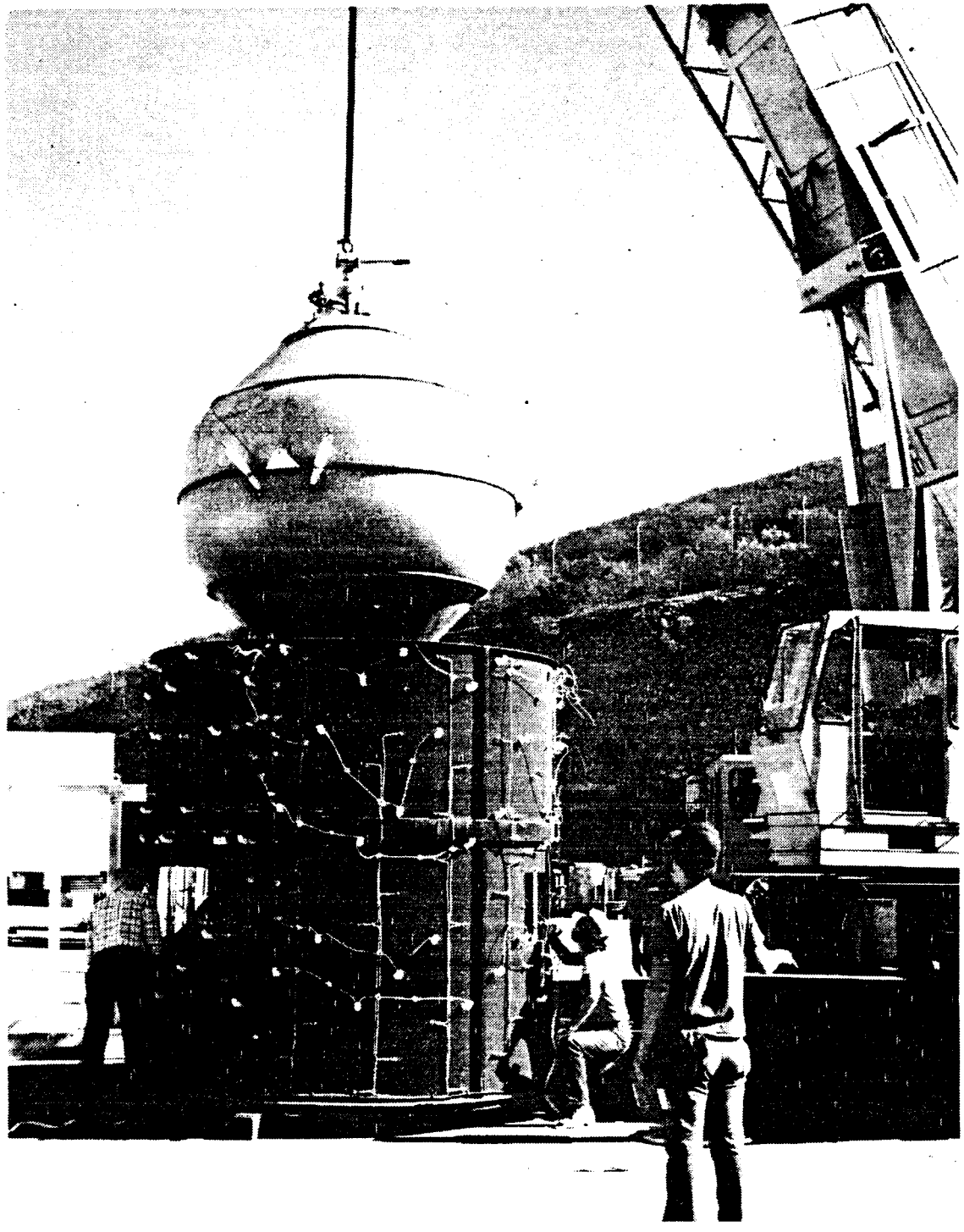

Figure 2-7. Test Article Being Installed in Enclosure

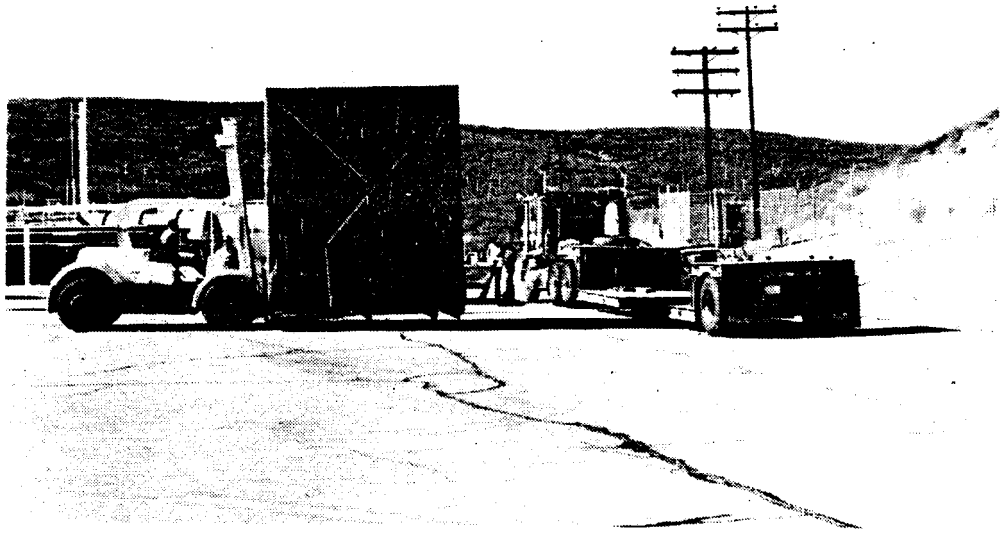

Figure 2-8. Test Article Being Loaded for Transport to MSFC

SECTION 3

START BASKET PERFORMANCE ANALYSIS

3.1 INTRODUCTION

The Cryogenic Breadboard Tank system is equipped with a start basket liquid acquisition device. The function of this device is to provide restart propellants to the engines of a vehicle operating in the zero-gravity environment of space, without the need for propulsive settling. It is located near the tank outlet and is designed to contain sufficient propellant to allow the engines to start and operate until the bulk liquid settles to the bottom of the tank. During engine burn the basket refills for the next coast/restart cycle. The start basket boundary consists of fine mesh screen which allows liquid to pass through the walls when the engines are operating, but prevents liquid from escaping from the basket during periods of zero-g coast.

3.2 DESIGN AND EXPECTED PERFORMANCE

The General Dynamics-built start basket was tested in the 2.2-m (87-in.) diameter CBT at the Marshall Space Flight Center between June 18 and June 24 of 1984. Figure 3-1 shows the test timeline. Testing was essentially continuous from the beginning of test #1 to the end of test #10. The test fluid was liquid hydrogen and the pressurants used were gaseous hydrogen and helium. Although hard vacuum was not achieved in the chamber, heat leak into the tank was not large enough to affect the results of the tests.

The purpose of the test series was to prove the concept of a start basket capillary liquid acquisition device using a multi-screen liner in conjunction with a single-screen window. Figure 3-2 is a schematic cross section of the start basket and inner acquisition channels, and Figure 3-3 is a photograph of the same components. The multi-screen liner is specifically designed to provide high heat flux interception capability, minimize wicking distances to prevent screen dry out, and preferentially allow vapor to penetrate the device while maintaining overall retention capability. For the device to function as designed, the pressure inside the start basket must fluctuate as cycles of vapor penetration and liquid resealing occur at the window screen to accommodate the evaporation occurring at the outer basket screen. A simplified schematic of the start basket configuration and a representative inner volume pressure trace are shown in Figure 3-4. Details of development work and scaled testing of a similar device were reported in Ref. 10.

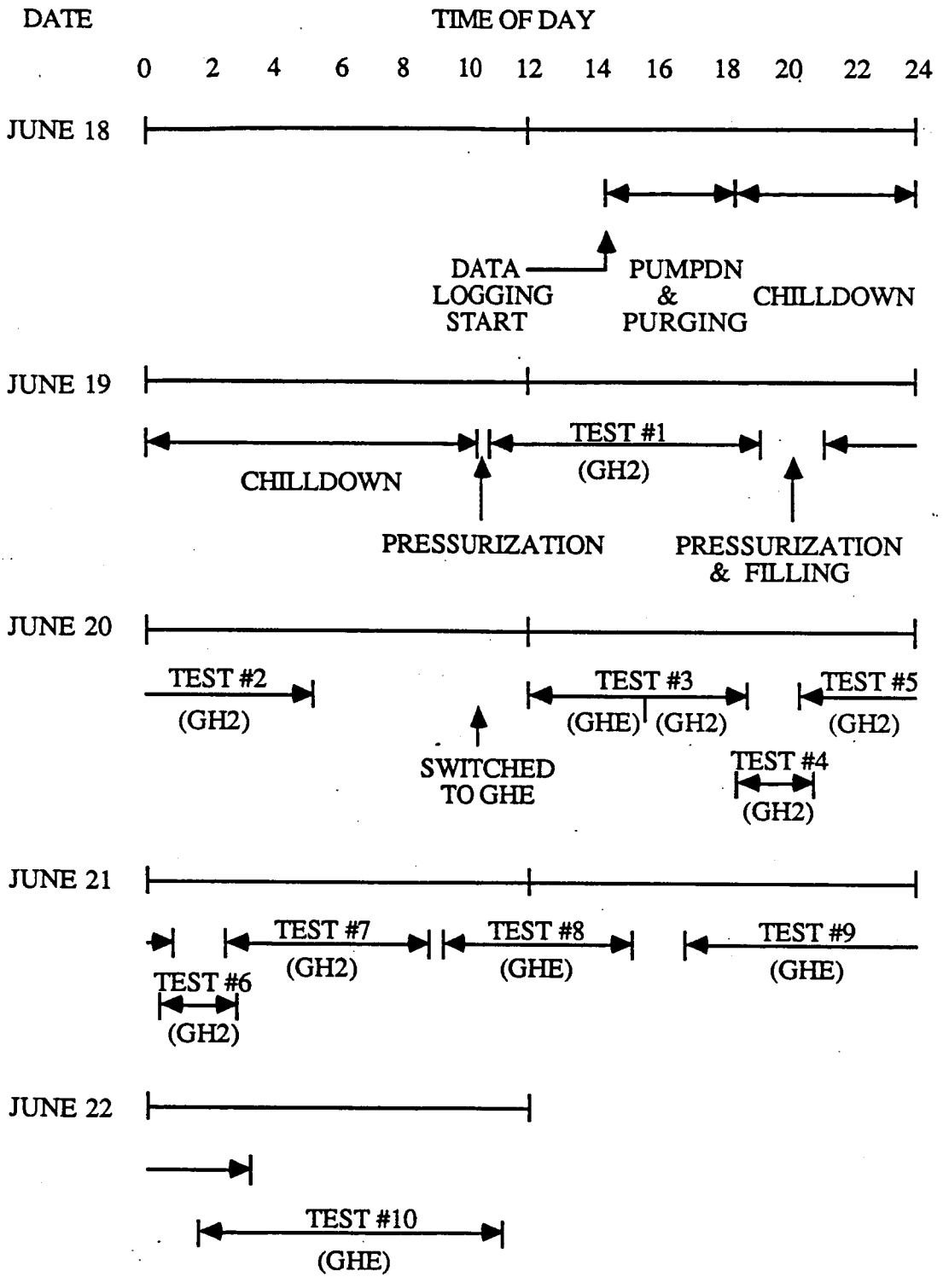

Figure 3-1. Start Basket Test Timeline

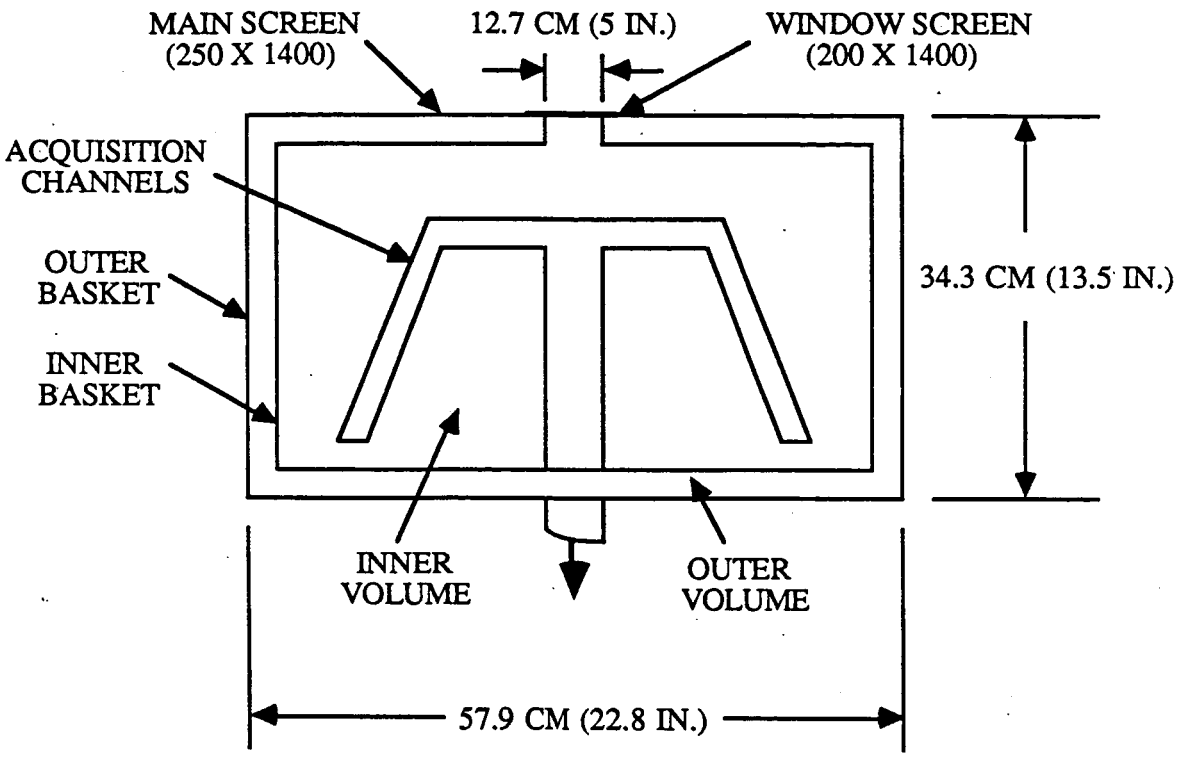

Figure 3-2. Start Basket Cross Section Schematic

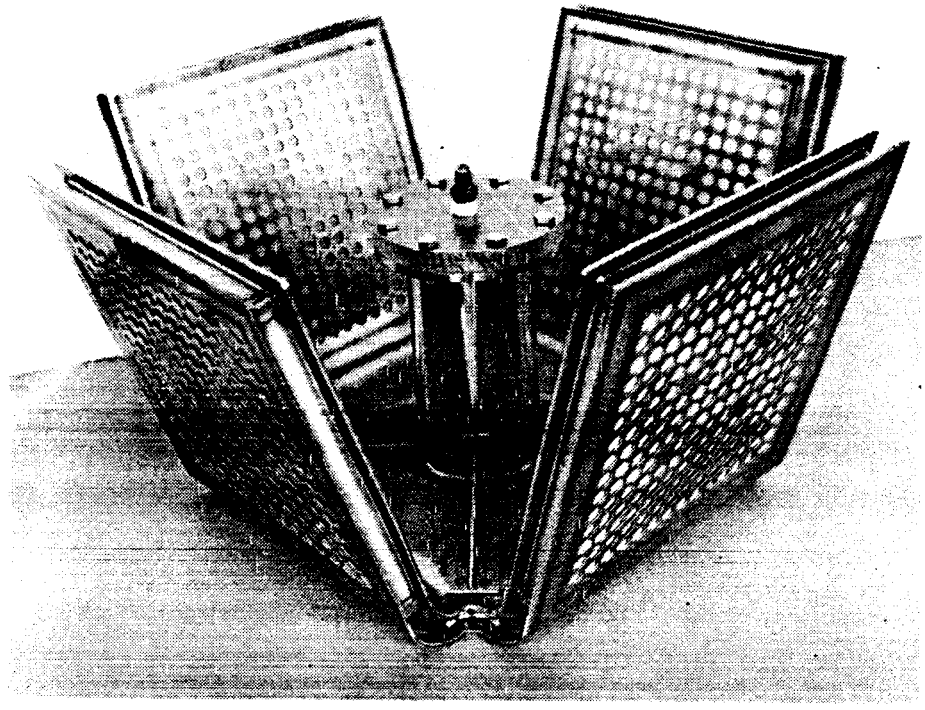

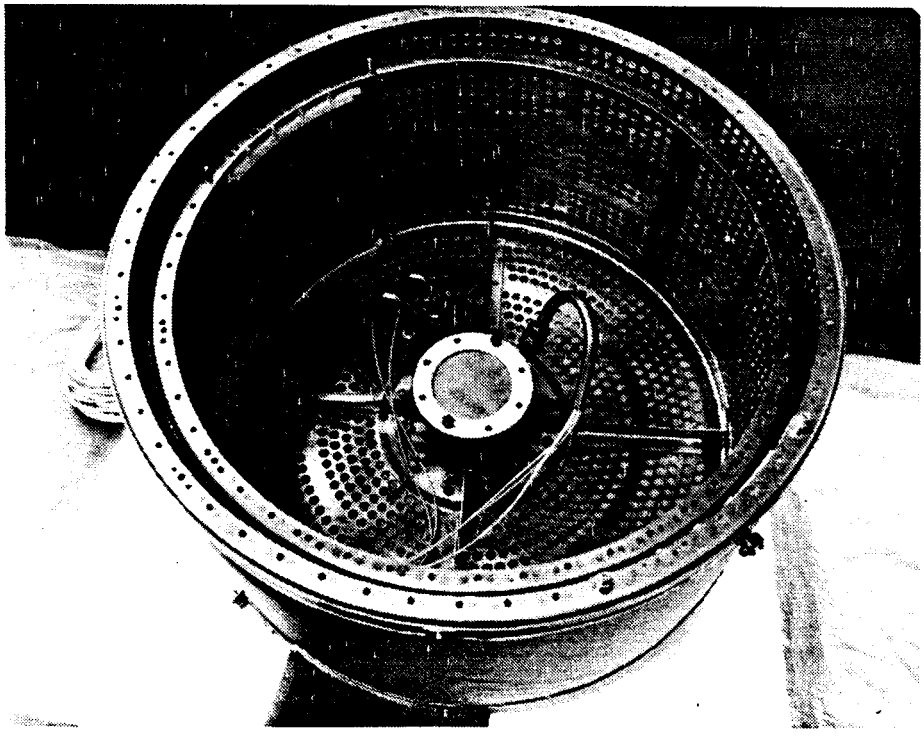

Figure 3-3. Photographs of Start Basket Components

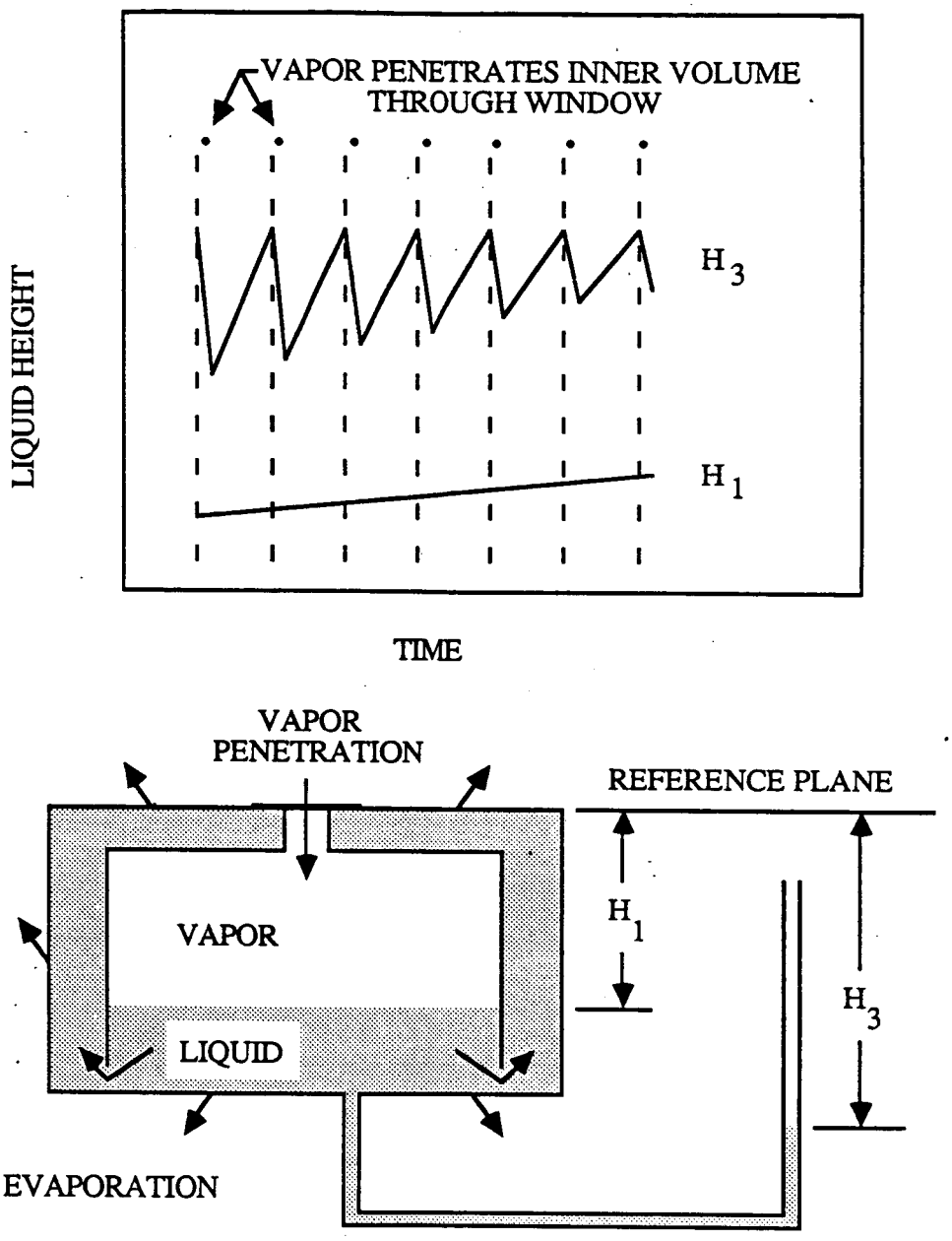

Figure 3-4. Schematic of a Window Screen Start Basket Device and Pressure Fluctuations

A standard test with the CBT start basket consists of the following:

1. Fill the basket by raising the tank liquid level above the top of the basket
2. Drain the liquid in the tank until the liquid level drops below the bottom of the basket
3. Allow the system to stand as liquid evaporates from the outer screen of the basket.
4. Monitor liquid levels and pressure inside the basket.

If the device works as expected, results of the test are:

1. Cyclic vapor penetration and liquid resealing at the window screen, and internal pressure fluctuations similar to those shown in Figure 3-4.
2. Periodic liquid level decrease in the inner volume of the basket.
3. No liquid level decrease in the outer volume until all the liquid in the inner volume is depleted.

Start Basket

The expected performance is based on the basket design. The liquid hydrogen retention height capabilities of the fine mesh screens used in the basket, as determined by bubble point measurements, are

Main	250 x 1400	61 cm (24 in.)
Window	200 x 1400	53 cm (21 in.).

The window screen with its lower retention capability allows vapor to preferentially enter the inner volume replacing the liquid evaporated from the outer main screen surfaces. The height of the basket, 34.3 cm (13.5 in.), was selected to make the maximum possible hydrostatic head in the basket only slightly more than one-half of the retention pressure, or head, of the main screen. The size of the window screen was selected to be capable of resealing in the presence of heating rates up to 13 W/m^2 (4 Btu/hr ft^2).

Test Results

The test configurations and maximum liquid retention heights for the ten test runs are summarized in Table 3-1. The results indicate that the start basket did not perform as expected.

Table 3-1. Summary of Start Basket Tests

Test No.	Pressurant	Tank Fill Time min.	Maximum Retention Height cm (in.)	Remarks
1	GH2	5	0	
2	GH2	10	0	
3	GHe/GH2	12	34.3 (13.5)	Held 30 min.
4	GH2	32	24.1 (9.5)	
5	GH2	15	33.8 (13.3)	
6	GH2	20	30.5 (12.0)	
7	GH2	22	30.5 (12.0)	
8	GHe	18	34.3 (13.5)	Held for 3 hours
9	GHe	21	34.3 (13.5)	Held for 60 min.
10	GHe	35	34.3 (13.5)	Failure in outer volume only

The observed results can be separated into two broad categories. The first is premature retention failure of the basket screen, and the second is failure of the window screen to reseal. Premature retention failure was observed during seven of the test runs. No evidence of window screen resealing was observed during any of the runs. Once vapor penetrated the window screen into the inner volume, or through the main screen into the outer volume, draining of the basket was continuous until the basket was essentially empty. Most of the time the two liquid levels, inner and outer volumes, dropped almost simultaneously. Failures in the remaining three runs occurred after the basket had maintained 34.3 cm of retention, the design limit.

Six of the seven test runs that exhibited premature failure employed gaseous hydrogen pressurization; the seventh used helium. The three test runs that showed the maximum possible retention of the basket, but failed during the refill cycle, were performed with helium pressurization. Therefore, although the window screen system did not breakthrough and reseal as expected, the data indicate that the start basket exhibited better retention characteristics in the presence of the helium pressurant. Of the six failures with GH_2, two runs (1 and 2) showed virtually no liquid retention. This premature retention failure will be referred to as mode 1.

Retention failure designated mode 2 was seen in test runs 3 and 9. During these tests the tank was drained down below the bottom of the basket and held at this condition for 30 minutes and 60 minutes, respectively. No breakdown occurred until the ensuing tank refill cycle was initiated. Liquid level and tank pressure traces for tests 3 and 9 are shown in Figures 3-5 and 3-6. Note that a relatively large pressure spike occured in test 9 at the time refill was initiated.

Retention failure mode 3 was exhibited in runs 4 through 7, where the tank was pressurized with hydrogen. During these runs the basket lost liquid during the initial tank drain operation. The maximum retention height at the time of the failure varied from 24 cm (9.5 in.) to 34 cm (13.3 in.) in run 5.

Retention Failure

Retention failure mode 1 was observed during test runs 1 and 2. Here cold hydrogen gas, at approximately 89 K (-300 F), was used to pressurize the tank. During both runs, the liquid levels in the basket compartments exhibited instability. The level in the outer volume started to fall before that of the inner volume. During test run 1, the data indicated that the outer volume began falling when the tank liquid level was above the top of the basket (Figure 3-7). This mode of failure is only possible when a sizeable vapor trap is formed in the basket volumes during the initial fill operation. Retention failure was evident both at the main screen of the outer basket and at the window screen. Liquid levels of both the inner and outer volumes generally moved downward side by side with the tank liquid level.

In preparation for the tests, the tank was filled with liquid hydrogen through the fill/drain line. During this operation the liquid level in the tank is always higher than the levels in the basket volumes. The magnitude of the differences depends on the tanking rate. When the liquid level in the tank rises rapidly, the difference is greater, and *vice versa*. When the liquid level in the tank rises above the top of the basket and wets the screen on the top, gas bubbles can be trapped inside the basket. If the quantity of gas trapped under the screens is such that the required wicking length exceeds the critical wicking length, the screens will dry out and breakdown will occur. The sizes of the bubble traps which occurred during the tests are not known.

The durations of the fill operations were 5 and 10 minutes for test runs 1 and 2, respectively. These fill times were the shortest of the ten runs, suggesting that larger bubble traps may have been generated during these two runs. To check the assumption of a bubble trap, a plastic box

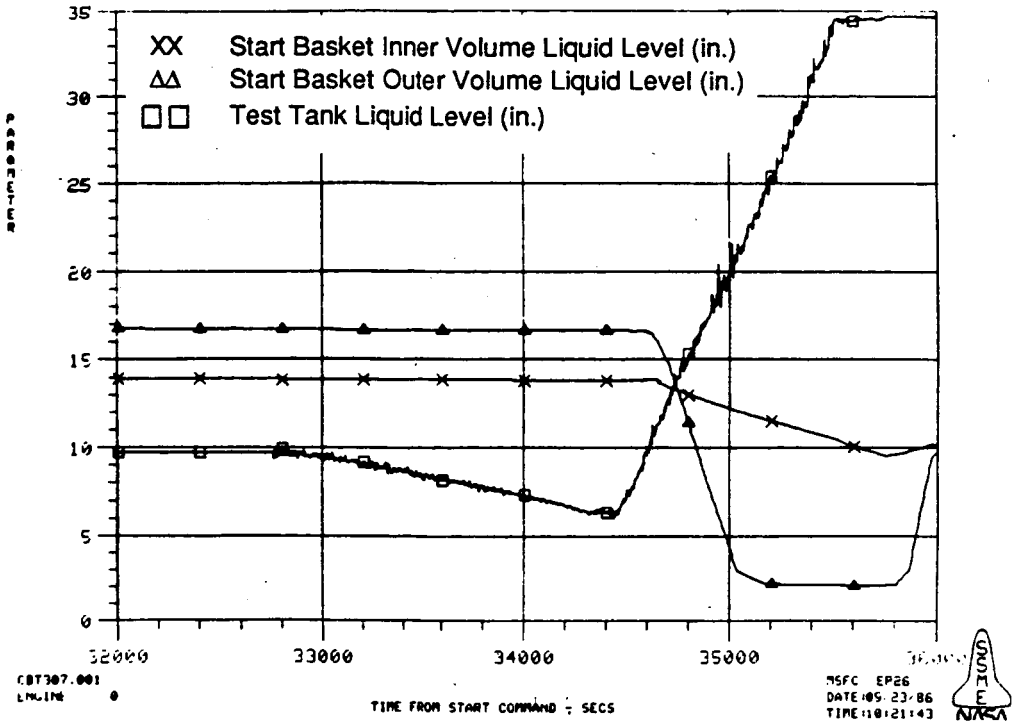

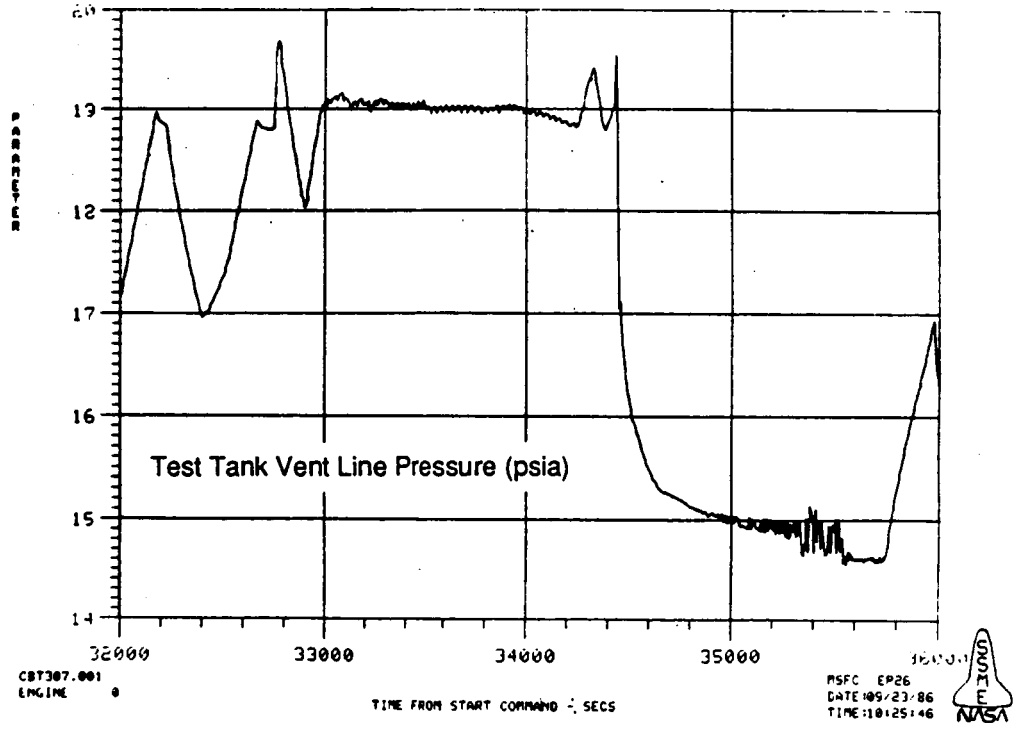

Figure 3-5. Tank liquid level and pressure traces for test 3.

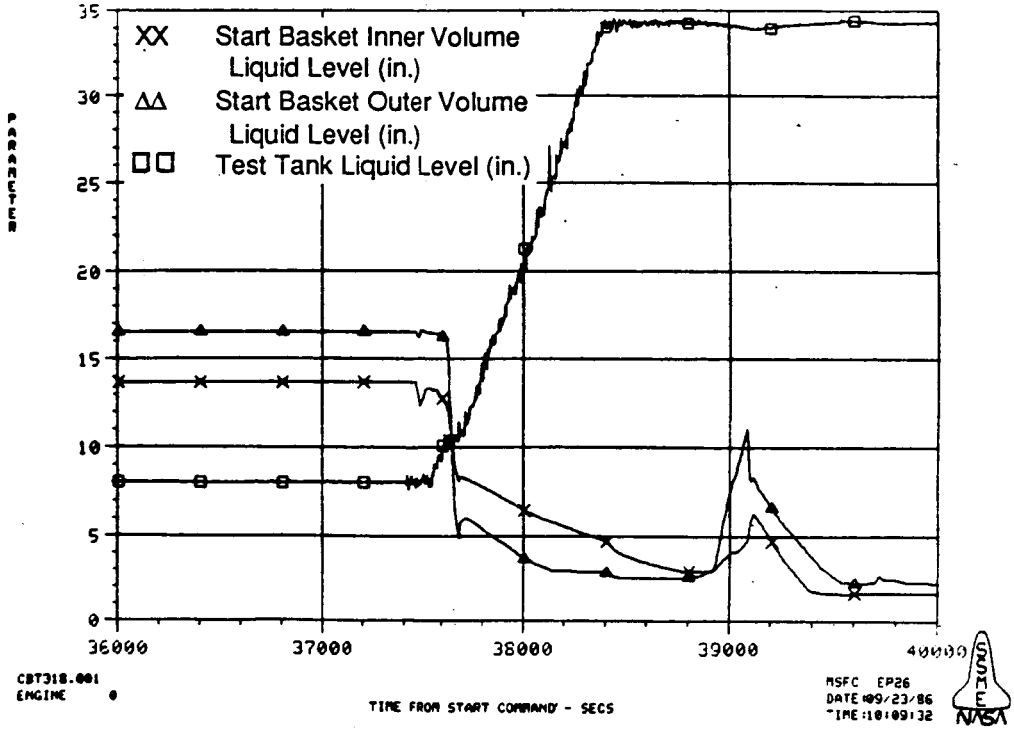

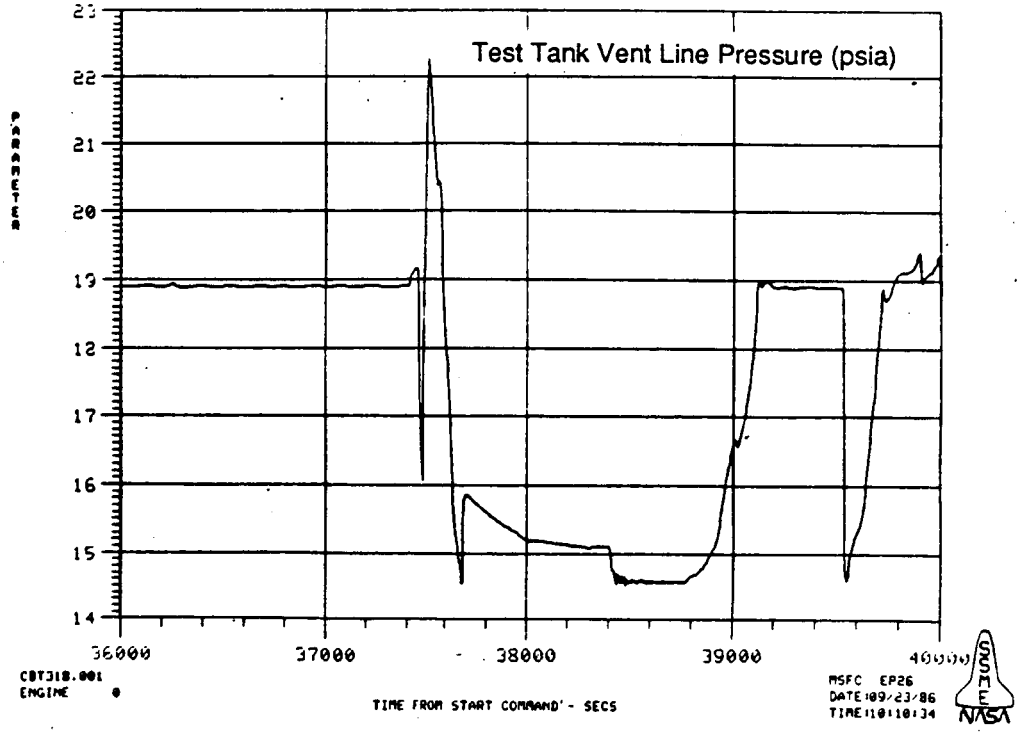

Figure 3-6. Tank liquid level and pressure traces for test 9.

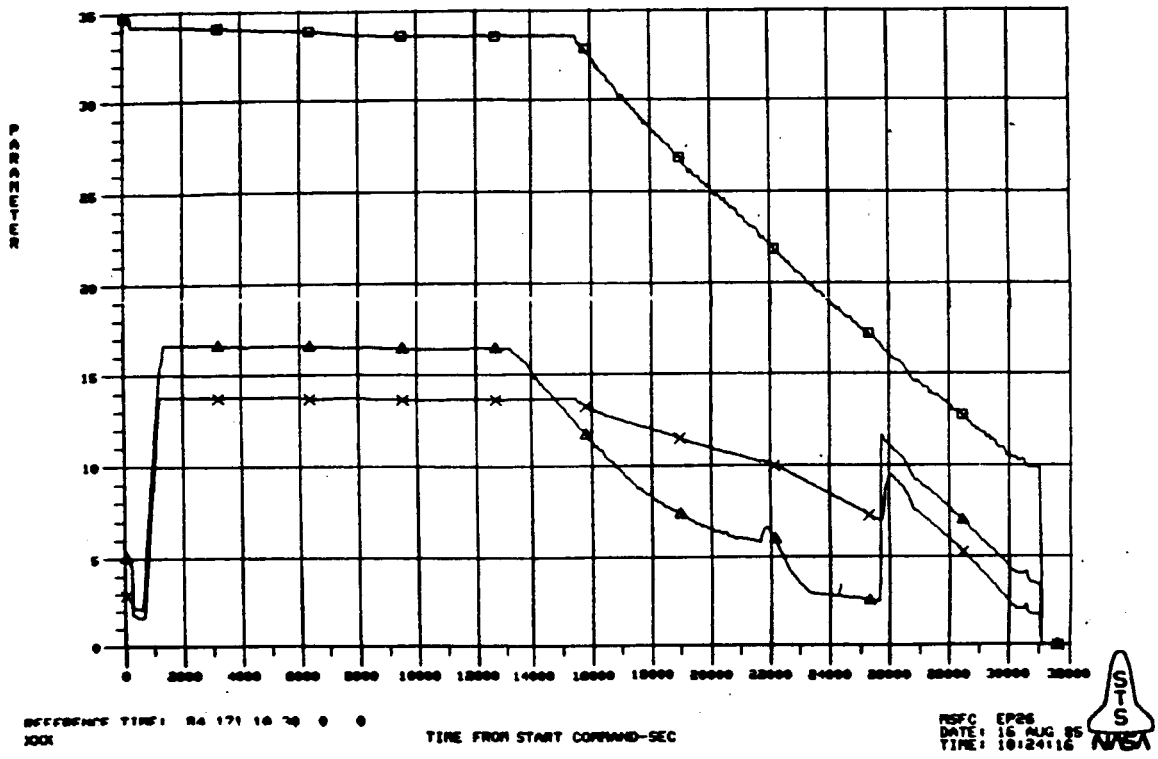

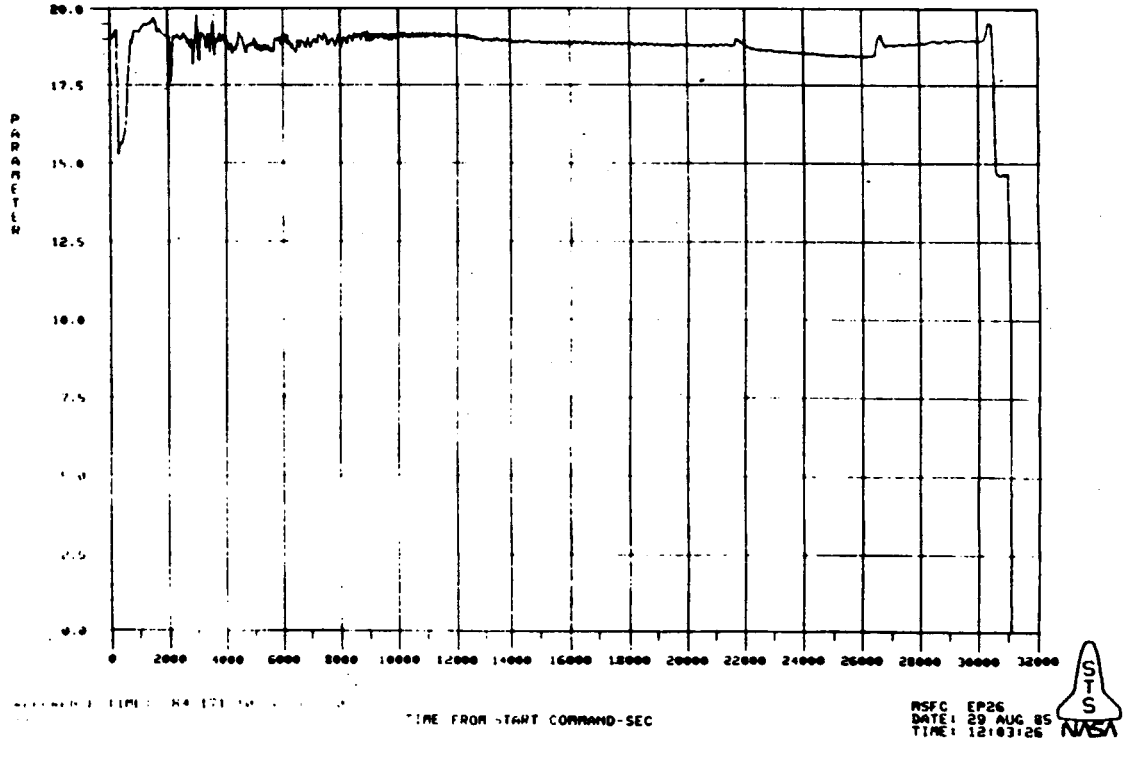

Figure 3-7. Tank liquid level and pressure traces for test 1.

with 200 x 1400 screens was slowly lowered into an alcohol bath. This test did not simulate the CBT fill operation quantitatively due to differences in screen mesh and fluid surface tension; however, it did graphically demonstrate the trapping of gas inside the device. It was found to be very difficult to completely fill the box without trapping some vapor. Complete filling could only be achieved by jiggling the box toward the end of the fill operation.

The effect of the type of pressurant gas on the existence of the bubble trap and the consequent retention failures was examined. Considering the mechanism which is believed to cause vapor trapping, the type of pressurant should have no effect on the quantity of vapor trapped. The test runs 1 and 2, used hydrogen as the pressurant. However, the same results would likely have occurred had helium been used as the pressurant. The temperature of the pressurant should also have no effect on vapor trapping. The type of pressurant gas and its temperature will, however, have a significant effect on how quickly the screen dries out.

The minimum size of the bubbles which can bring about the kind of failure observed in runs 1 and 2 is estimated from the dry out length of the screens. For the horizontal screens of mesh size 200 x 1400 (window) and 250 x 1400 (main), dry out lengths of 3.6 and 3.8 cm (1.4 and 1.5 in.) were calculated based on a design heat flux of 13 W/m^2 (4 Btu/hr ft^2). Vapor traps of these sizes, 7.2 and 7.6 cm (2.8 and 3.0 in.), equal to twice the dry out length since wicking will occur from both sides, would seem to be possible unless extreme care is taken during tank fill to avoid them.

For a space vehicle using a start basket LAD, liquid orientation prior to engine restart is a function of the various acceleration forces imposed on the vehicle during the coast phase. Even the small magnitude drag and reaction control forces will affect liquid positioning. As the relatively large axial acceleration force of engine restart is imposed, the liquid in the tank will settle to the bottom, possibly forming a geyser as the fluid moving down the walls meets near the outlet. Considerable agitation of the liquid could result. The effect that this type of motion may have on the ability of the start basket to be refilled without significant vapor trapping is unknown.

Possible scenarios for failure mode 2, seen in runs 3 and 9, have been examined. In this mode, the failures take place between the time when refilling starts and tank liquid level reaches the bottom of the basket. The time scale used to generate the liquid level data plots was such that an accurate assessment was not possible. The failure took place approximately 25 to 50 seconds from the time the tank liquid level reached the bottom of the basket. Another interesting

phenomenon common to both runs was tank pressure spikes measured at the time refilling started. Two candidates for the cause of mode 2 failure are 1) tank liquid level touching the basket and 2) pressure peaking.

The basket at the time of refilling was under some strain because evaporation had occurred at the outer wall but no pressure relief had occurred at the window screen. When the basket contacts the liquid bath the strain may suddenly be relieved as the pressure difference causes liquid to rush into the basket. The flow transient may have degraded the retention capability of the screen and caused the failure. The suspected pressure peaks were reviewed. The pressure peaks, 2.1 - 6.9 kPa (0.3 - 1.0 psi), lasted for only a few seconds. However, these peaks are much larger than the maximum screen retention capability, 345 Pa (0.05 psi), and could be a cause of vapor penetration. With this magnitude of pressure differential, breakdown can take place anywhere along the basket wall. It also appears to be possible that breakdown could lag the actual spike. Assuming tank pressure quickly returns to its starting value at the termination of the spike, the screens should rewet sealing the basket interior and preventing liquid fallout. Then it is only after the injected vapor reorients within the basket to form large, or larger, vapor pockets that dry out, and total breakdown, will occur.

Possible causes of the sudden pressure jumps were examined. Refilling is accomplished by opening the fill valve and introducing colder, subcooled liquid into the fill system. The subcooled liquid expands to a lower pressure and boils in the warmer fill/drain line when refilling starts, causing a sudden pressure change. The two causes can also be related. When the cold liquid is introduced into the tank at high velocity, the liquid can splash and come in contact with the basket.

Failure mode 3 could be due to the presence of small bubbles trapped under the screen. Failure may result when the sizes of the bubbles grow and exceed the window screen wicking capability during the draining process. Heat fluxes at the basket wall are estimated to range between 3 and 16 W/m^2 (1 and 5 Btu/hr ft^2) based on measured temperature gradients and assumptions regarding natural convection heat transfer coefficients. At heat fluxes of this level, dry out is not expected unless a significant bubble trap is formed. The growth of the trapped bubble could be accelerated due to basket heating and liquid vapor pressure reduction in the inner volume of the basket.

Resealing

Preferential vapor penetration and liquid resealing was expected on the window screen, but this is only possible when the outer basket volume is filled with liquid hydrogen. For most of the runs, the inner and outer volume liquid level drops were almost simultaneous, indicating retention failure at both the main and window screens. A few of the runs exhibited failure first at the main screen. As was discussed in the basket retention failure review, bubble trapping was the most likely cause of this failure. If this is the case, preferential penetration at the window screen will not occur. This was clear from the test results.

The resealing process was examined with a capillary model built with plastic and tested in alcohol. Results of this study are presented in Appendix I. This study suggests that resealing is not possible when the fine mesh screen internal pore size is much larger than the external pore size. For a few of the screens tested, the internal pore was found to be larger than the external pore. The internal pore is not as easy to characterize as the external pore. However, this work strongly suggests that resealing may not be possible at all for certain fine mesh screens. If screen dry out occurs due to vapor trapping, and the screen internal pore size is larger than the external, resealing would not be expected to occur.

SECTION 4

RELATED LIQUID ACQUISITION DEVICE STUDIES

4.1 INTRODUCTION

A thorough understanding of the retention characteristics of fine mesh screens and the mechanisms that enhance or degrade retention is essential for the proper design of liquid acquisition devices using such screens. The terms enhance and degrade are meaningful only when the standard retention capability of a screen/liquid combination is properly established. Some of the confusion in the assessment of screen retention capability comes from the lack of understanding of the pertinent phenomena and the standard procedures used to measure screen retention capability.

Capillary retention is achieved when a wet screen separates a liquid from a gas at a higher pressure, or the wet screen separates two gases at different pressures. The maximum pressure differential before a gas bubble penetrates into the liquid side in the first case, or the maximum pressure difference the wet screen can maintain without allowing vapor to pass in the second case, is called the retention capability or the "bubble point." The screen in the first case will be referred to as a main screen, while that in the second case will be called a communication, or window screen (Figure 4-1).

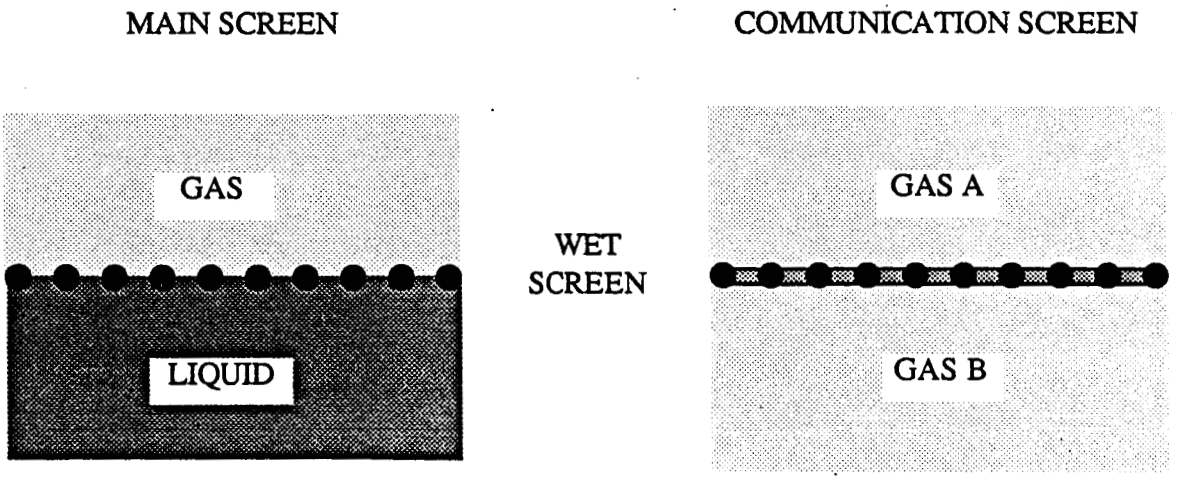

Figure 4-1. Schematic of Main and Communication Screens

The bubble point of a screen/liquid combination is determined experimentally. The experiment establishes screen parameters such as bubble point diameter, D_{BP}, and wicking constant, ϕ. The bubble point of a given screen combined with different liquids can be calculated using these parameters. The most commonly used technique to determine bubble point is to position a screen horizontally with a thin layer of liquid on top and an enclosed gas volume beneath. An alternate technique with the liquid on the bottom is shown in Figure 4-2.The gas pressure the the enclosed volume is then gradually increased until a bubble is observed at the liquid side of the screen. The maximum pressure before the bubble breaks through is called the bubble point pressure. The bubble point of a given screen is a function of surface tension of the liquid in the pores. The pore size varies across the screen sample, and the initial break through takes place where the pore is largest. Thus any large defective pores uncharacteristic of the screen must be sealed prior to the test.

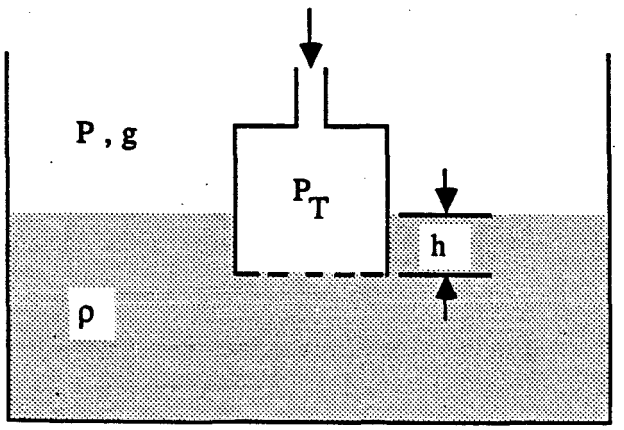

$$\Delta P_\sigma = P_{Tc} - (P + \rho g h)$$

P_{Tc} is the critical P_T at which the first bubble is observed.

Figure 4-2. Bubble Point Measurement Test Setup

Irregular pore sizes and the lack of standard measurement procedures are partially responsible for differences in reported bubble point values for the same screens. The bubble point measurement must be carried out such that both heat and mass transfer between the screen and pressurant are minimized. High heat transfer combined with a low vapor pressure can generate a bubble at the liquid side of the screen which can be mistaken for vapor penetration. The liquid film in the screen pores can be heated or cooled depending on the mode of heat and mass

transport at the screen. Some of the observed degradation may be attributed to unrecognized temperature changes. Heat transfer may dry out the liquid film in a communication (gas/gas) screen causing premature failure.

The relationship between the bubble point, ΔP_σ, and the screen/liquid parameters is generally expressed as

$$\Delta P_\sigma = \phi \sigma / D_{BP}$$

This equation suggests that the bubble point is determined by screen and liquid parameters only, and is independent of the type of pressurant gas. D_{BP} and ϕ are considered constants and ΔP_σ is a function of the wetting liquid surface tension only.

Surface tension of the wicking liquid is that of the liquid in the screen cavities and not that of the bulk liquid. This distinction is crucial because the temperature of the liquid in the screen pores is sensitive to the heat and mass transport at the screen/vapor interface and may be different from that of the bulk. This is especially true when the ullage pressure is raised prior to outflow. The temperature of the bulk liquid would not change immediately, but the temperature of the liquid in the screen would quickly rise to achieve thermodynamic equilibrium with the adjacent vapor. The surface tension of liquid hydrogen decreases by as much as 25 percent with a temperature rise of 2.8 degrees Celsius. The percent change in surface tension is illustrated in Figure 4-3.

The capillary wicking constant, ϕ, reflects a deviation of screen pore shape from the ideal circular pore. For a circular capillary tube and zero contact angle, it is 4.0. For the screen, it is determined experimentally in conjunction with the pore diameter, D_{BP}. The pore diameter is calculated using the number and diameter of the wires in the screen, and reflects the square root of average cross-sectional area of the pores. When D_{BP} of the screen is thus determined, the wicking constant is calculated from

$$\phi = \Delta P_\sigma D_{BP} / \sigma.$$

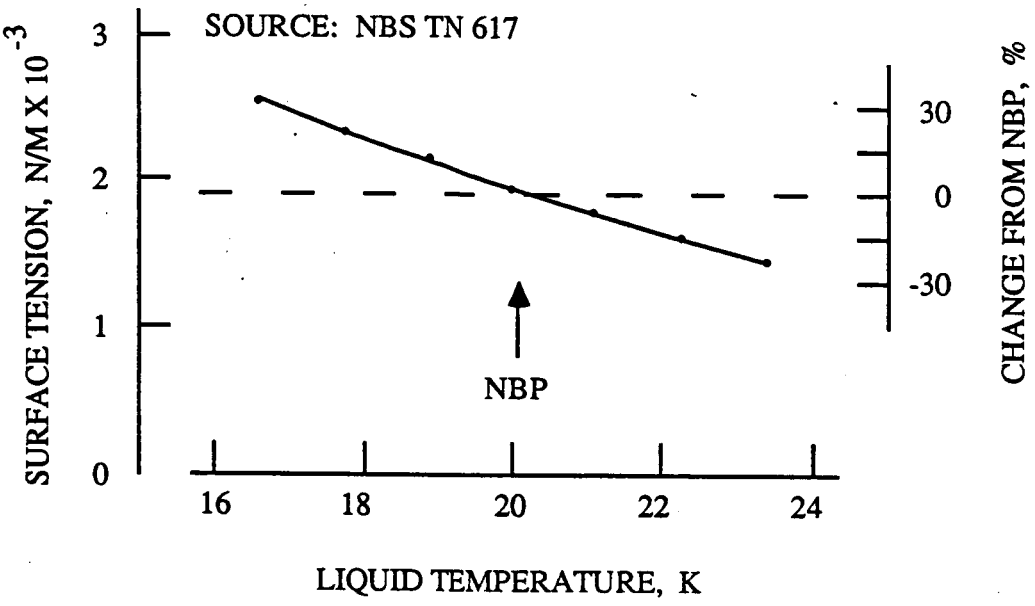

Figure 4-3. Liquid Hydrogen Surface Tension Variation

4.2 PARAMETERS AFFECTING SCREEN RETENTION

The retention capability of a screen depends on a number of parameters:

Pressurant	a) type of gas
	b) gas temperature
	c) gas motion
	d) degree of saturation, or partial pressure
Screen	a) type - main or communication
	b) orientation
	c) weave direction
	d) wettability/contamination
Liquid	a) stagnant or in motion
	b) degree of subcooling
Other	a) vibration

Not all of these factors affect the retention capability of a screen in a given device. The effect of each will be discussed in general terms and then will be related to previous studies.

Pressurant

As is clear from the ΔP_σ correlation, the type of pressurant should not directly affect the retention capability of the screen. Rather, it affects ΔP_σ through heat and mass transport. Choice of pressurant affects heat and mass transfer in a number of ways. Warm autogenous pressurant may condense on the screen, raise the screen temperature, and degrade retention capability. A non-condensible pressurant can reduce local partial pressure and thereby promote stronger evaporation, lowering the screen temperature and enhancing retention capability of a main screen (by increasing liquid surface tension). The same pressurant for a communication screen will cause premature breakdown if the screen wicking ability is not sufficient to match the rate of evaporation, especially when the screen is oriented vertically. The combination of high heat transfer, low vapor pressure, and a non-condensible pressurant may cause boiling on the liquid side of the main screen. This could then lead to screen dry out and premature failure.

For a given pressurant, a lower gas temperature always results in higher retention performance. Pressurant motion in close proximity to the screen affects heat and mass transport and screen retention capability. For non-condensible gas pressurization cases, the ullage is made up of two gases and it is generally not fully saturated. The degree of saturation of the ullage and the choice of pressurant therefore will affect heat and mass transfer at the screen/ullage interface.

Severe bubble point degradation when warm pressurant was used was reported by Burge and Blackmon (Ref. 3) during their 250 x 1370-mesh screen bubble point measurement tests. Warm GH_2 was blown against a screen holding liquid hydrogen. Screen retention capability degraded rapidly as gas temperature and heat transfer increased. The gas temperature ranged between 33.3 and 54.7 K (60 and 98.5 R) and the heat transfer coefficients between 45 and 74 W/m^2 K(8 and 13 Btu/hr ft^2 R). The resulting heat fluxes were found to be between 322 and 1610 W/m^2 (102 and 510 Btu/hr ft^2). Bubble point degradation of the magnitude found in the Ref. 3 study may not result from a single cause; however, screen dry out should be suspected when the heat flux is greater than 315 W/m^2 (100 Btu/hr ft^2).

Liquid acquisition tests with an Interface Demonstration Unit reported in Ref. 4 revealed that both warm hydrogen and helium caused a marked decrease in effective screen bubble point; however, the effect was greater with warm hydrogen. The strong degradation with hydrogen may be attributed to the high heat transfer due to hydrogen vapor condensation on solid portions of the device.

The effect of pressurant temperature on screen retention performance was also observed during a minus one-g expulsion test (Ref. 5). The tank was pressurized with either hydrogen or helium at various temperatures. While most of the tests were successful, a few of the multiple expulsion tests with warm hydrogen pressurant showed evidence of screen dry out. Screen dry out and breakdown generally occurred within a few seconds of outflow termination. Dry out was never experienced with the helium pressurant. Considering that the warm pressurant was directed onto the top of the manifold, it is possible that the manifold was heated above the liquid saturation temperature. When the outflow terminates, the excess enthalpy is absorbed by the stagnant liquid generating vapor in the outflow manifold. As was seen in the Ref. 4 tests, warm hydrogen condensing on the manifold could have raised the manifold temperature more than did the warm helium pressurant.

The above examples indicated that warm hydrogen pressurant degrades the performance of a liquid hydrogen screen acquisition device more than does warm helium. The screens for the above cases were main screens (liquid/gas). Opposite results were seen when the screen was a communication screen. During expulsion tests with a subscale liquid hydrogen model (Ref. 6), the pressure difference histories across the communication screen were noticeably different for the two pressurants, hydrogen and helium. For the helium tests, the maximum retention pressure difference was less than that measured during the hydrogen tests, and breakdown occurred much more quickly with helium than it did with gaseous hydrogen. Evidently the reduction of the hydrogen partial pressure caused by the introduction of helium increased the rate of evaporation of liquid from the screens and accelerated dry out..

Screen

The choice of screen mesh and the number of layers of screens determine the maximum retention capability available for an acquisition device. It is the design application of the screen, however, which determines whether the available retention is fully used. A screen may be used as a main screen or a communication screen. Multiple main screen layers are known to improve retention capability. However, full advantage will be realized only when a proper gap is

maintained between the screen layers. While performance of a main screen is not greatly affected by how it is used, performance of a communication screen is very sensitive to the design application due to relatively easy screen dry out.

For the main screen, wicking capability is not an important consideration, but it is of critical importance for a communication screen. Although weave direction of a main screen is not important to it's retention performance, it can again be of crucial importance for a communication screen. Wicking capability is known to be greater in the direction perpendicular to the shute wires. The weave direction of a communication screen should be chosen such that the maximum wicking capability is utilized. Orientation affects retention performance of a main screen very little, but it is an important consideration for a communication screen. Proper choice of weave direction becomes especially important when the wicking direction of the screen is against a gravity gradient.

The wicking capability of a screen is especially important when warm gas is used for the pressurization of cryogenic propellant tanks. Available information concerning screen wicking capability is somewhat limited. Ref. 7 examined wicking as a solution to the problem of evaporation from a screen device. Ref. 8 presented an analysis of wicking data for a single test conducted with 375 x 2300 mesh dutch twill screen. Results of a most extensive study on wicking rate were presented in Ref. 9. As a part of the study, an analytical model was developed which expresses the wicking velocity as a function of various system parameters. The experimental data were compared with the model to determine geometry constants.

The most important requirement for a communication screen is the capability to stay wet and maintain a continuous liquid film to prevent vapor flow through the screen. To stay wet, it must be able to reseal by wicking after the liquid film in the screen is broken due to an excessive pressure differential across the screen. The second requirement for a communication screen is to stay wet in the presence of evaporation. The referenced studies were concerned with the wicking rate of screens. The ability of a communication screen to reseal is examined in Appendix I.

Liquid

Surface tension is the one liquid property that directly affects screen retention capability. However, the liquid can affect retention in more than one way. Liquid in motion can convey heat away from areas of high heat flux thereby reducing the danger of vapor generation which

degrades retention capability. During liquid outflow through the device, the liquid is in motion and screen breakdown may not be noticed. At termination of outflow, when the liquid is stagnant, it may boil inside the device to degrade the retention. The degree of subcooling of the bulk liquid can also affect screen retention capability. A cryogenic liquid storage tank is normally charged to a pressure slightly above one atmosphere, but the pressure is raised during acquisition and transfer to subcool the liquid and prevent flashing in the acquisition device and the transfer line.

Other

Vibration and flow transients have been known to affect screen retention performance. For vibration, the effects of amplitude, frequency, and screen mesh size on capillary stability have been examined. Experimental models have been mounted on shaker tables and subjected to both random and sinusoidal vibration in directions both normal and parallel to the screen surface. A flow transient study defined the severity of a flow transient which results in a destabilization of the liquid/vapor interface at the screen surface and vapor ingestion into the liquid. Warren (Ref. 5) examined the effects of the two phenomena on screen retention performance.

The vibration study showed that the performance of a capillary liquid acquisition device can be predicted using hydrostatic theory for wide band random vibration; that is, gas ingestion will occur when the pressure difference due to static and dynamic flow exceeds the screen bubble point. For the flow transient study, unsteady pressure simulating startup and shutdown was applied and its effect on breakdown examined. Although the test results were inconclusive, the following guidelines were recommended:

1. Screen material should have a bubble point in excess of 5.0 kPa (20 in. of water)
2. Channel velocity should not exceed 0.2 m/s (0.66 ft/s)
3. Screen/liquid contact area should be maximized.

SECTION 5

CONCLUSIONS AND RECOMMENDATIONS

Zero-gravity capillary liquid acquisition devices have been under investigation for more than twenty years. The space shuttle orbital maneuvering and reaction control systems successfully employ such devices for acquiring and transferring storable propellants in space. However, questions remain concerning the viability of capillary devices for use with cryogenic liquids on space-based orbital transfer vehicles and propellant storage depots. This contract provided data which was helpful in increasing understanding of the phenomena which characterize cryogenic LAD performance. However, additional study is required to investigate the microscopic aspects of cryogenic liquid retention and breakthrough/resealing, particularly in conjunction with incident heat flux and tank pressurization. Other types of capillary barriers may provide improved internal/external pore characteristics and overall retention performance than do fine mesh screens. In light of the significant advances being made in precision manufacturing techniques, it is recommended that a program be initiated to study alternatives to screens for LADs.

SECTION 6

REFERENCES

1. K.E. Leonhard, Develop and Demonstrate the Performance of Cryogenic Components Representative of Space Vehicles, Phase I Report, CASD-NAS78-009, General Dynamics Convair Division, Contract NAS8-31778, November 1978.

2. C. Bassett *et al*, Develop and Demonstrate the Performance of Cryogenic Components Representative of Space Vehicles, Phase II Report - Integrated Systems Design and Analysis, GDC/NAS79-003, General Dynamics Convair Division, Contract NAS8-31778, March 1980.

3. G.W. Burge and J.B. Blackmon, Study and Design of Cryogenic Propellant Acquisition Systems, Final Report, MDC G5038, McDonnell Douglas Astronautics Co., Contract NAS8-27685, December 1973.

4. J.B. Blackmon, Design, Fabrication, Assembly and Test of a Liquid Hydrogen Acquisition Subsystem, MDC G5360, McDonnell Douglas Astronautics Co., Contract NAS8-27571, May 1974.

5. R.P. Warren, Acquisition System Environmental Effects Study, MCR-75-21, Martin Marietta Corp., Contract NAS8-30592, May 1975.

6. H.L. Paynter, Acquisition/Expulsion System for Earth Orbital Propulsion System Study, Final Report, Vol. III, NASA CR-134154, Martin Marietta Corp., Contract NAS9-12182, October 1973.

7. M.H. Blatt, J.A. Stark, and L.E. Siden, Low Gravity Propellant Control Using Capillary Device in Large Scale Cryogenic Vehicles, GDC-DDB-70-006, General Dynamics Convair Division, Contract NAS8-21465, August 1970.

8. Low-G Fluid Behavior and Control, R-71-48631-003, Martin Marietta Corp., 1971.

9. E.P. Symons, Wicking of Liquid in Screens, NASA TN D-7657, NASA/Lewis Research Center, May 1974.

10. M.H. Blatt and J.A. Risberg, Study of Liquid and Vapor Flow Into a Centaur Capillary Device, NASA CR-159657, General Dynamics Convair Division, Contract NAS3-20092, September 1979.

APPENDIX I

SCREEN RESEALING ANALYSIS

This appendix contains a detailed development of the equations governing vapor breakthrough and subsequent resealing in an idealized model of fine mesh screen pores. It was hypothesized that window, or communication, screen behavior is dependent on both an external pore diameter, which governs screen bubble point, and an internal pore diameter, which maintains liquid within the screen and governs when resealing will occur. Based on this hypothesis, an idealized model was developed which takes the physical form of two parallel plates with concentric holes of radius r, separated by a small gap, g. Surface tension forces fail to seal the holes when a critical pressure across the plates develops and vapor penetration occurs. The smaller gap between the plates retains liquid and, as the internal pressure rises, this liquid flows into the hole and seals the pore.

Several observed phenomena are explained by this model. Most notably the model indicates that pore resealing will not occur unless the gap is properly sized and the internal liquid pressure is sufficiently large, regardless of how small the pressure difference across the plates becomes. Furthermore, the resealing phenomenon is found to be very sensitive to fluid contact angle. Unless the contact angle is very small, resealing will not occur.

The problem was approached by assuming the pore is initially sealed and then progressively increasing the pressure differential until breakthrough occurs. Similarly, resealing was analyzed by progressively reducing pressure differential. The analysis was further idealized by neglecting dynamic forces and by ignoring the difference between advancing and receding contact angle. The gap fed pore model for resealing is shown in Figure I-1.

Breakthrough

Starting from an initial stage when $P_a = P_u$, the ullage pressure may be gradually lowered by draining from the bottom of the box. Draining simulates evaporation at the screen device surfaces. The various stages of screen breakthrough and resealing are examined below.

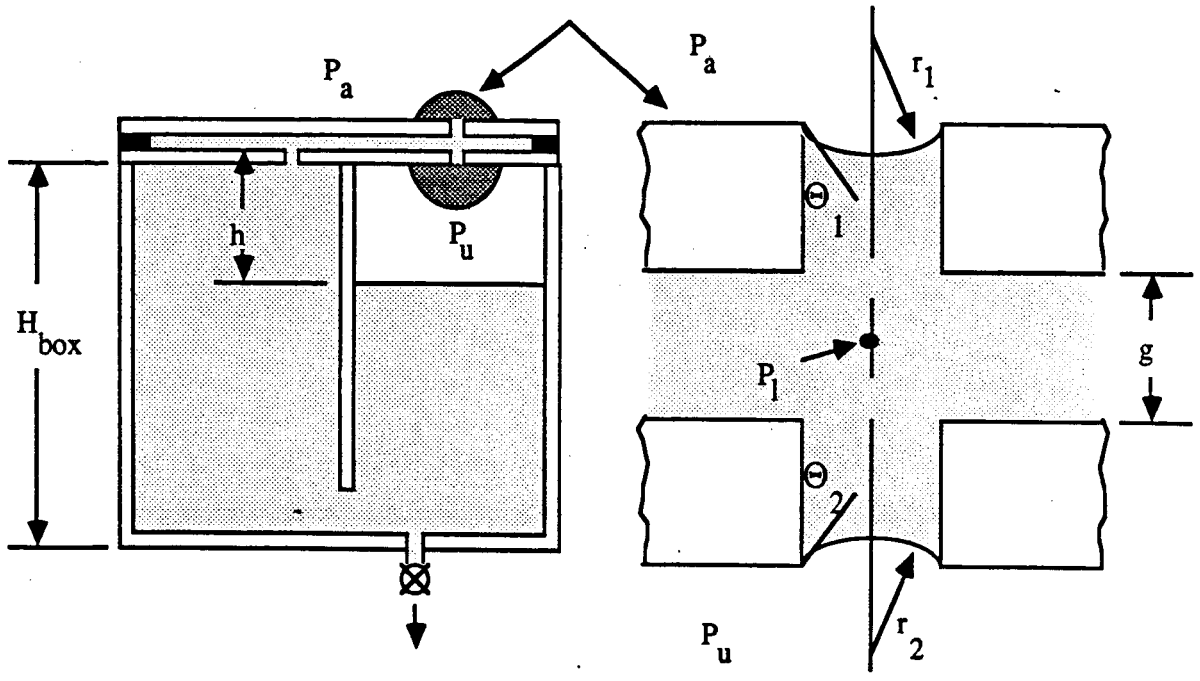

g	Gap width	r_1	Upper interface curvature
P_a	Ambient pressure	r_2	Lower interface curvature
P_u	Ullage pressure	r_3	Gap interface curvature
P_l	Liquid pressure	ΔP_u	$P_a - P_u$
Θ_1	Upper interface contact angle	ΔP_l	$P_u - P_l$
Θ_2	Lower interface contact angle	Θ	Liquid contact angle
		H_{box}	Height of box

Figure I-1. Gap Fed Pore Model

1) Stage 1

$$P_a = P_u > P_l \ , \ r_2 = r_1 > r \ , \ \Theta_1 = \Theta_2 > \Theta \ , \ P_u - P_l = \rho g h$$

2) Stage 2

This stage is reached when Θ_1 is reduced until $\Theta_1 = \Theta$. Then,

$$P_a - P_l = 2\sigma / r_1 = 2\sigma / r \cos\Theta.$$

This is an unstable point for the upper interface. An attempt to further decrease P_u and thus P_l will result in downward movement of the upper interface, pushing liquid through the gap.

3) Stage 3 (Figure I-2)

This stage is reached if P_u is further lowered until $r_1 = r$ and $P_a - P_l = 2\sigma / r$.

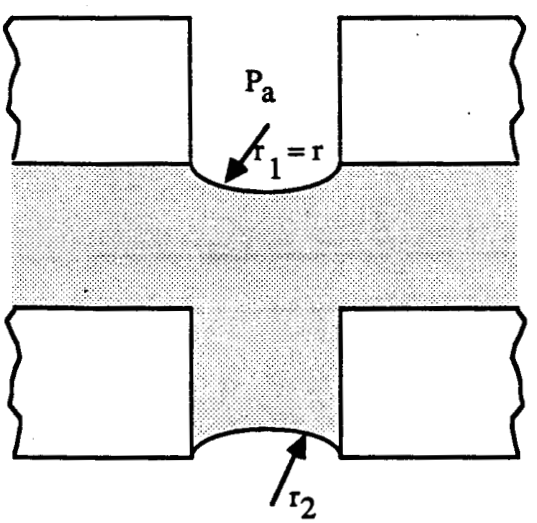

Figure I-2. Breakthrough Stage 3

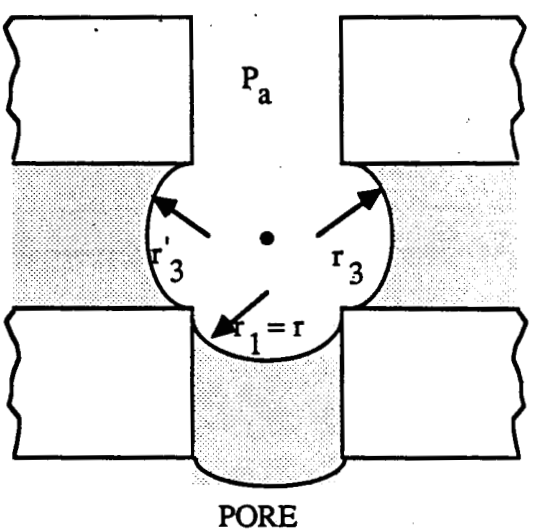

Figure I-3. Breakthrough Stage 4

4) Stage 4 (Figure I-3)

When the interface reaches this stage, the vapor can penetrate through either the pore or the

gap. The vapor will push through the interface whose retention ΔP is smaller.

Gap: $\Delta P_\sigma = \sigma (1/r_3 + 1/r) = \sigma (2\cos\Theta/g + 1/r)$

Pore: $\Delta P_\sigma = 2\sigma/r (\cos\Theta + \sin\Theta)$

For cryogenic liquids, $\Theta \approx 0$. Then

Gap: $\Delta P_\sigma \approx \sigma (2/g + 1/r)$

Pore: $\Delta P_\sigma \approx \sigma (2/r)$

If $g/2 = r$ Gap $\Delta P_\sigma \approx$ Pore ΔP_σ

If $g/2 < r$ Gap $\Delta P_\sigma >$ Pore ΔP_σ, and vapor will push through the pore

If $g/2 > r$ Gap $\Delta P_\sigma <$ Pore ΔP_σ, and vapor will push through the gap.

When the gap ΔP_σ is less than the pore ΔP_σ, the gap will dry out before the vapor penetrates through the gap. If this happens, resealing will be impossible.

Resealing following breakthrough

Pore breakthrough takes place when

$$P_a - P_u = 2\sigma/r (\cos\Theta + \sin\Theta) = \Delta P_\sigma$$

The resealing process following breakthrough is examined below

1) Stage 1 (Figure I-4)

The pressure difference across the gap interface is

$$P - P_l = \sigma (1/r_3 + 1/r)$$

$$= \sigma (2\cos\Theta_3 / g + 1/r)$$

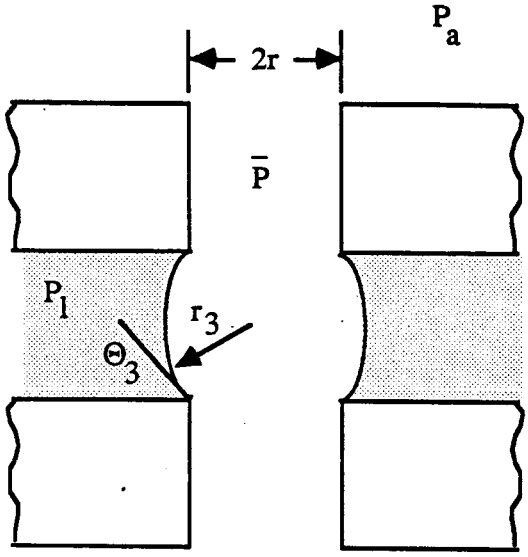

Figure I-4. Resealing Stage 1

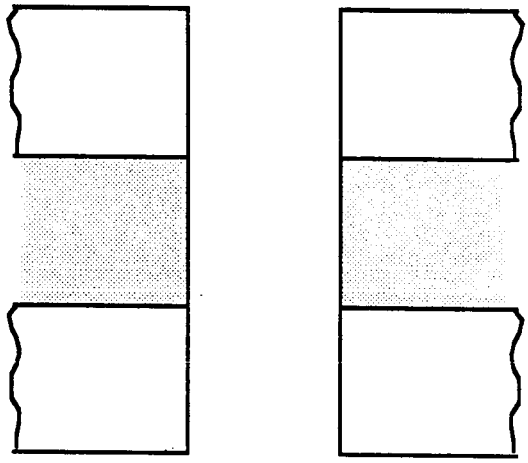

Figure I-5. Resealing Stage 2

2) Stage 2 (Figure I-5)

$P - P_l$ is reduced as P_l increases. This stage is reached when $r_3 = \infty$ and

$$P - P_l = \sigma / r$$

The limiting value of $P - P_l$ is

$$P - P_l = P_a - P_l = \rho g h$$

where h is the ullage height in the window screen compartment (Figure I-1).

3) Stage 3 (Figure I-6)

When $P - P_l < \sigma / r$, rewetting starts and

$$P - P_l = \sigma (1/r - 1/r_3)$$

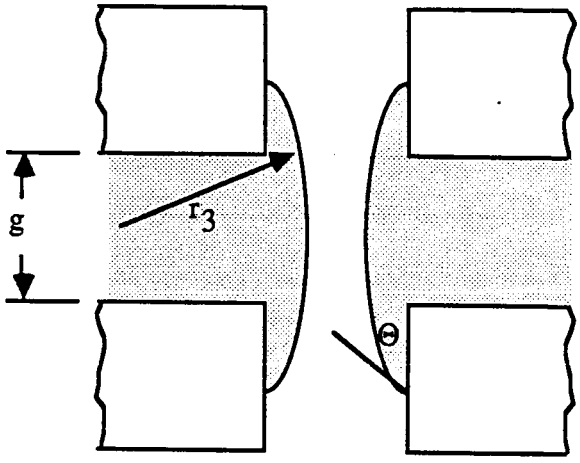

Figure I-6. Resealing Stage 3

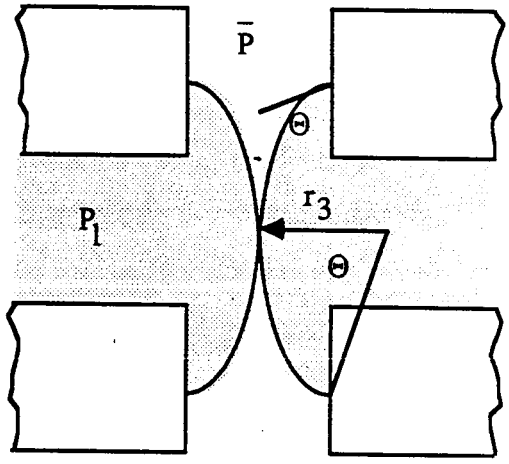

Figure I-7. Resealing Complete

4) Stage 4 (Figure I-7)

Resealing will be completed when $r_3 = r / (1 - \cos\Theta)$, such that

$$P - P_l \leq \sigma \cos\Theta / r$$

Letting $P = 0.5 (P_a + P_u)$, then

$$\begin{aligned} P - P_l &= 0.5 (P_a + P_u) - P_l \\ &= 0.5 (P_a - P_l) + 0.5 (P_u - P_l) \\ &= 0.5 \Delta P_u + \Delta P_l \end{aligned}$$

$$\therefore \Delta P_u \leq 2\sigma\cos\Theta / r - 2\Delta P_l$$

for resealing to be fully achieved.

Conclusions

1. The pore retention limit is

$$\Delta P_\sigma = 2\sigma / r\,(\cos\Theta + \sin\Theta)$$

2. The gap retention limit is

$$\Delta P_\sigma = \sigma\,(2\cos\Theta / g + 1 / r)$$

3. To keep the gap "full" up to the pore retention limit,

$$\Delta P_l = P_u - P_l = \rho g h < \sigma\,(2\cos\Theta / g + 1 / r) - 2\sigma / r\,(\cos\Theta + \sin\Theta)$$

That is, the gap retention limit should be greater than the pore retention limit for resealing.

4. The height of the box should be such that

$$\rho g H_{box} < 0.5\,\Delta P_\sigma$$

to achieve resealing when the liquid level in the box is very low ($h \approx H_{box}$).

Repeating the most critical conclusion, for resealing to be possible, the gap retention limit must be greater than the pore retention limit. The screen property which is equivalent to the gap retention limit can be obtained by dipping the screen in liquid and measuring the capillary rise height on the screen. Two sample screens were tested in alcohol and produced the following results:

Screen	External Pore Retention Limit	Capillary Rise Height
	cm (in.)	cm (in.)
2300 x 325	58 (23)	12.7 (5)
1200 x 250	46 (18)	11.4 (4.5)

Although these two parameters are not strictly comparable, the capillary rise height is proportional to the retention limit for the internal pores of the screen. It also follows that the greater the rise height, the smaller the internal pore diameter. Note also that the coarser screen has a smaller rise height, evidence of a larger internal pore size. These results suggest that for these screens, the gap or internal pore is larger than the external pore. The consequence is that resealing will be impossible once vapor penetration takes place. Although the start basket screens are different from those illustrated above, the test results in which resealing did not occur could be explained by the same screen internal/external pore effect discussed above.